https://journals.unizik.edu.ng/ujcee

Unizik Journal of Chemical & Environmental Engineering

Volume 1, Issue 1, Pages 001-014
2026

Received: 20.04.2026
Accepted: 02.06.2026
Published: 08.06.2026

Application of Clay-based Nanoparticles for Enhancement of Biogas Production from Anaerobic Co-digestion of Cow Dung and Yam Peels

Obioma E. Achugbu[1*], Joseph T. Nwabanne[1]
[1]**Department of Chemical Engineering, Nnamdi Azikiwe University, Awka, Nigeria.**
* Correspondence: oe.achugbu@unizik.edu.ng

Abstract
This work investigates the application of clay-based nanoparticles (CBNPs) for enhancing biogas production from anaerobic co-digestion of cow dung and yam peels. Locally-sourced clay lumps were crushed, pulverized, calcined in a muffle furnace at 700°C for 2 hours and treated with 1 M phosphoric acid (H_3PO_4) to enhance porosity. The synthesized CBNPs were characterized using Dynamic Light Scattering (DLS), Scanning Electron Microscopy (SEM), X-Ray Diffraction (XRD), Fourier-Transform Infrared Spectroscopy (FTIR), X-Ray Fluorescence (XRF) and Brunauer-Emmet-Teller (BET) techniques. The substrates, cow dung and yam peels, were sourced locally and equally characterized. A central composite design (CCD) within response surface methodology (RSM) was utilized to evaluate 20 experimental batch runs across three factors: time, substrate ratio, and nanoparticle concentration. DLS analysis confirmed the nanoscale structure, revealing a dominant particle size of 12.78 nm. BET results indicated a specific surface area of 204 m^2/g and mesoporous particles with favourable adsorptive properties. The characterization results of the substrates indicate complementary properties. Microbial assays on the cow dung confirmed the presence of active microorganisms essential for anaerobic digestion. The RSM quadratic model established predicted a maximum biogas yield of 2238.28 ml under optimal conditions of 11 days retention time, a 56% substrate mixing ratio (cow dung: yam peels) and a 151 mg/L NPs concentration. CBNPs addition significantly improved biogas yield and methane content by 24.5% and 4 % respectively, compared to the control. This enhancement is attributed to accelerated substrate degradation, improved electron transfer, and enhanced microbial activity.

Keywords: anaerobic digestion, cow dung, yam peels, clay, nanoparticles

Introduction

The search for more ecologically friendly and renewable energy sources has intensified due to the issue of global warming brought on us by the burning of conventional fuels. Additionally, the total amount of organic and solid waste produced is growing much more quickly and this can have negative impact on our globe if improperly handled (Abdelwahab, Mohanty, Sahoo, Behera and Fodah, 2021). Due to inadequate waste management methods in developing nations like Nigeria, large

volume of organic wastes, including cow dung, generated are allowed to putrefy, polluting the air and/ or water except in some cases where they are utilized as fertilizer. A study of Anambra State's main slaughterhouses revealed that 15563 kg (15.6 tons) of fresh cow manure are produced per day (Umeghalu, Chukwuma, Okonkwo and Umeh, 2012). In order to extract energy from organic wastes, waste-to-energy (WtE) systems such as anaerobic digestion are used. In a number of applications, WtE can be regarded as a semi-renewable energy source that can replace conventional fuels (Obaideen *et al.*, 2022). Anaerobic digestion is a technique for the management of urban and agricultural wastes. It is the most important biological treatment that produces a CH_4 by-product from organic matter (Abdelsalam *et al.*, 2019). According to Abdelsalam and Samer (2019), anaerobic digestion (AD) is a group of bioprocesses in which microorganisms biodegrade and transform organic materials into byproducts like biogas without the presence of oxygen. A group of microorganisms, including carbon dioxide-reducing methanogens, acetoclastic methanogens, hydrogen-producing and hydrogen-consuming acetogenic bacteria, and fermentative bacteria, are involved in the process (Lohani and Havukainen, 2018). In addition to producing biogas for energy and digestate as biofertilizer, anaerobic digestion enhances the aesthetics of our environment by promoting cleanliness and lessening the offensive odors from these wastes. Anaerobic digestion is a promising renewable energy source for producing biogas, however process constraints frequently impede its conversion efficiency, process stability, product quality, and economic viability.

To maximize the efficiency of anaerobic digestion, co-digestion - the simultaneous digestion of two or more substrates – is frequently employed. This strategy optimizes the complementary carbon-to-nitrogen (C/N) ratio within the bio-digester, which directly enhances cumulative biogas yields and maintains robust system stability under varying organic loading rates (Zhang, Xiao, Peng, Su and Tan, 2013). Yam peels are one of the agricultural wastes that are mostly disposed carelessly without any attempt to harness the bioenergy in them. They have high volatile solid content and high C/N ratio required to sustain the anaerobic microbes and hence, can be useful in biogas production especially by co-digesting with cow dung which has lower carbon content but in turn serves as the microbial consortium.

To further accelerate methane production, recent advancements have focused on the integration of advanced additives, specifically microelements or nanoparticles smaller than 100 nm (Khan and Hossain, 2022). The incorporation of these nanomaterials have been reported to significantly boost methane yields by disrupting the complex crystalline structure of lignocellulosic waste. This enzymatic disruption increases the bioavailability of fiber content, making it available to hydrolytic and methanogenic anaerobic bacteria (Ajayi-Banji, Pourhashem, Rahman and Feng, 2024). Under optimized operating parameters, addition of certain nanoparticles can enhance biogas production by some percentages, though experimental outcomes fluctuate depending on the specific nanoparticle morphology, core material and digester configuration (Castro, Resende, Taveira, Enrich-Prast and Abreu, 2024).

Biochemical acceleration of anaerobic digestion via nanotechnology is largely driven by three distinct mechanisms. Firstly, there is enhanced direct interspecies electron transfer (DIET). Conductive nanoparticles establish direct electrical pathways between syntrophic bacteria and methanogenic archaea, which drastically optimizes the rate-limiting steps of methanogenesis. Secondly, transition metal nanoparticles act as essential enzymatic co-factors, accelerating the metabolic pathways of crucial acidogenic and methanogenic populations. Thirdly, clay-based nanoparticles provide a high surface area protective matrix for microbial immobilization. This framework reduces the toxic shock of inhibitory compounds (such as volatile fatty acids and ammonia) by providing stable adsorption sites.

However, the performance of these nanoparticles is influenced by several factors, including particle size, concentration, pH, and substrate composition (François, Lin, Rachmadona and Khoo, 2023). Excessive concentrations of nanoparticles frequently trigger cellular toxicity, leading to disruption of microbial cell membranes and the complete inhibition of crucial methanogenic communities. Consequently, establishing precise operational thresholds is paramount to balancing performance enhancement against catastrophic system destabilization (Passalacqua, Collina, Fullana and Mezzanotte, 2024).

This underscores the importance of determining optimal nanoparticle dosages to balance performance enhancement with system stability. There is equally a lack of integrated studies that simultaneously optimize key process parameters such as retention time, nanoparticle concentration, and substrate ratio, particularly in co-digestion systems involving locally available feedstocks such as yam peels. Also, it was not found reported in any previous research of the use of locally-sourced clay nanoparticles for anaerobic co-digestion of yam peels and cow dung. Hence, this work aims at exploring this and obtaining optimal nanoparticles concentration.

2.0 Materials and Methods

2.1 Materials

Local clay was collected from Nteje in Oyi Local Government Area, Anambra state, South-East of Nigeria, The cow dung was collected from cattle market at Ugwuoba Garki, Enugu State while the yam peels were obtained from a restaurant at Ifite, Awka metropolis, Anambra State, Nigeria. The chemicals used were obtained from Bridge head market Onitsha and Chemical Engineering Laboratory, Nnamdi Azikiwe University, Awka, Anambra State, Nigeria and were of analytical grade.

2.2 Methods

2.2.1 Preparation of the Substrates

Fresh wet cow dung and yam peels were used for this work. The yam peels were first washed with distilled water to remove the dirt in them. They were then ground to paste with a mechanical grinding machine and was ready for characterization and anaerobic digestion.

2.2.2 Preparation of CBNPs

The method reported by Teğin and Saka (2023) was employed with slight modifications. The clay lumps were pulverized and was washed with deionized water to remove impurities. The sample was dried in an electrical oven at 100–120°C to eliminate moisture. It was then treated with 1 M of phosphoric acid (H_3PO_4) to enhance porosity. The sample was heated in the muffle furnace at 700°C for 2 hours to activate the clay structure. It was left to cool to obtain the clay-based nanoparticles (CBNPs).

2.2.3 Characterization of the Substrates and CBNPs

The proximate analyses of the substrates were done using AOAC methods while the physicochemical properties were analyzed using standard laboratory methods. The morphology of the CBNPs were examined using SEM while XRF analysis was carried out for elemental composition. In addition, BET was carried out to obtain the specific surface area, DLS for the particle size distribution, FTIR for the functional groups present and XRD, to evaluate the crystalline structure of CBNPs.

2.3 Batch anaerobic digestion experiment

Table 1 shows the upper and lower limits that were set for the factors. It shows a range of 3 factors used in the experiment. These factors with their selected ranges were used to predict the response which is the biogas yield and to determine the model that best fits the data.

Central Composite Design (CCD) of the Design Expert software was used to generate the Design of Experiment (DOE) (Table 2) which involves 20 runs. The factors are A-time (days), B-NPs concentrations and C-Substrates ratio while the response is the biogas yield (Y).

Fresh cow dung (CD) and yam peels (YP) were first mixed in different volume ratios with the addition of nanoparticles to obtain 800 mL of substrate. Following the method described by Farghali *et al.* (2020), this substrate was mixed with 800 mL of distilled water to achieve a 1:1

substrate-to-water ratio. The resulting 1.6 L slurry was introduced into a 3 L plastic biodigester with a headspace of 1.4 L. The setup was replicated for 20 runs and the biogas yield was measured by downward displacement of water in a measuring cylinder and recorded on a daily basis. Additionally, a digester consisting of 400 mL of CD and 400 mL of YP mixed with 800 mL of water was equally set up as a blank or control (without nanoparticles).

Table 1: Parameters and their Levels for the Biogas Process from CCD

Factor	Name	Units	Minimum	Maximum	Coded Low	Coded High	Mean	Std. Dev.
A	Time	Days	3.95	14.05	-1 ↔ 6.00	+1 ↔ 12.00	9.00	2.54
B	NPs conc.	mg/L	65.91	234.09	-1 ↔ 100.00	+1 ↔ 200.00	150.00	42.39
C	Substr. ratio	%	7.96	92.04	-1 ↔ 25.00	+1 ↔ 75.00	50.00	21.20

Table 2: Design of Experiment (DOE) for the batch experiments

Run	A:Time (Days)	B:Nano. conc (mg/L)	C:Substr. ratio (%)	Biogas yield (ml)
1	12	200	75	
2	12	100	75	
3	6	200	75	
4	9	150	50	
5	6	200	25	
6	12	100	25	
7	6	100	75	
8	9	150	50	
9	9	150	8	
10	9	150	50	
11	6	100	25	
12	4	150	50	
13	9	66	50	
14	12	200	25	
15	9	150	50	
16	9	150	50	
17	9	150	92	
18	14	150	50	
19	9	234	50	
20	9	150	50	

3.0 Results and Discussion

3.1 Characterization Results of CBNPs

3.1.1 FTIR of CBNPs

The spectrum shown in Table 3 confirms that CBNPs is a clay sample. Strong Si–O stretching at ~1027–1038 cm^{-1}, Al–O/Si–O bending around ~670 cm^{-1}, and structural OH stretching in 3400–3700 cm^{-1} region, collectively confirm an aluminosilicate clay mineral system. Clay minerals (kaolinite, illite, smectite), were present. In agreement with the results obtained in Jozanikohan and Abarghooei (2022), the FTIR spectrum confirms a mineral composite consisting of: clays/aluminosilicates (Al-OH, Si-O-Al), quartz/silica (Si-O-Si) and metal oxides (Al, Fe).

The spectrum shows that CBNPs has good potential to enhance methane yield in anaerobic digestion. Surface hydroxyls provide anchor points for anaerobic microbes, especially methanogens, increasing digestion efficiency. On the other hand, aluminosilicates and silica are chemically stable and mildly alkaline. They can adsorb acids produced during hydrolysis/acidogenesis and consequently prevent pH drops that inhibit methanogens (Tzenos *et al.*, 2023). This brings about stability in the anaerobic environment with improved methane yield. Metal oxides containing iron and aluminum can serve as trace nutrients for the microbes. They can equally facilitate DIET in syntrophic reactions, enhancing conversion of VFAs to methane as posited in (Park, Kang, Park and Park, 2018; Vannarath *et al.*, 2025). Clay-silica matrix presents high surface area due to the layered structure of clay. This increases adsorption of organics and make them available for the microbes. The substrate is thus concentrated at the microbial surface and the digestion efficiency is increased. Silicate and hydroxyl-rich surfaces can adsorb toxic compounds like ammonia or sulphides, and thus, reduce inhibition of methanogens.

Table 3: Peak, intensity and Assignments of FTIR analysis of CBNPs

S/N	Observed Wavenumber(cm^{-1})	Intensity / Peak Shape	Functional Group	Vibrational Mode	Bond Nature / Remark
1	3689.67	Strong, sharp	O–H (alcohol/phenol)	Asymmetric stretching	Inner surface hydroxyl groups
2	3619.33	Strong, Sharp	O–H group	symmetric stretching	Non-hydrogen bonded hydroxyl groups
3	1113.69	Medium, sharp	Si-O	Longitudinal stretching	SiO_2 or free quartz
4	1027.41	Strong, broad	Si-O-Si	In-plane stretching	General clay backbone
5	1003.24	Strong, Sharp	Si-O-Al	Asymmetric stretching	Pure kaolinite clay mineral
6	910.58	Strong, sharp	Al-OH	Bending/deformation	Kaolinite structural hydroxyl groups
7	787.79	Medium	Si-O-Si stretching	Symmetric stretching	Indicates quartz, silica
8	749.89	Medium	Si-O-Al	Symmetric stretching	Al incorporated into the framework
9	672.83	Weak/Medium	Si-O-Si/Si-O-Al	Bending/mixed ring	Internal linkage deformation
10	530.51	Strong/Medium	Si-O-Al/Si-O	Bending	Aluminosilicate layers

3.1.2 SEM-EDS

The SEM micrograph of CBNPs is presented in Plate 1. The micrograph done at (320x, 15kV)

reveals a heterogeneous and porous microstructure. It has fine grains, abundant irregular porosity. The dispersed bright particles indicate the presence of heavy minerals. Numerous dark regions correspond to pores. The vein-like structures shows that there were particle packing. The plate-like arrangement of micro-sheets is characteristic to kaolinite. Interstitial voids and open channels in the spaces between the folded stacks and micro-sheets act as the primary physical transport network. The large surface area visible in the micrograph confirms that CBNPs has a high density of active sites available to adsorb and neutralize the inhibitors in the systems. The clustered aggregates help to bind dispersed bacterial cells and loose substrates together into dense microbial flocs. This improves the biogas production.

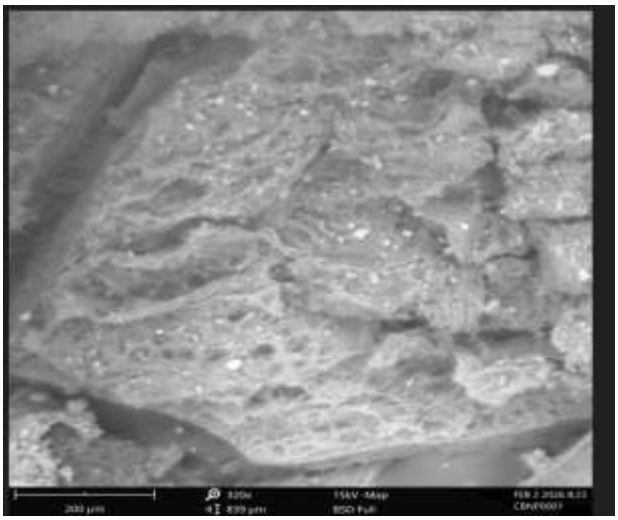

Plate 1: SEM micrograph of CBNPs

3.1.3 XRD of CBNPs

The XRD results of CBNPs is presented in Figure 2. The XRD of CBNPs exhibits a pattern with sharper, more intense, and more numerous diffraction peaks, alongside a less pronounced amorphous hump. This indicates a high degree of crystallinity and a well ordered mineral structure. The identified features suggest the presence of nacrite (kaolin group clay mineral, polymorph of kaolinite), muscovite (illite/mica group) which confirms the clay-rich nature and these are phyllosilicates with characteristic layered structures. Nacrite ($H_4Al_2Si_2O_9$) is the less common polymorph of the kaolin group. It typically forms under higher temperature/pressure conditions or specific hydrothermal environments compared to kaolinite. The features equally shows the presence of orthoclase (K-feldspar) and albite (Na-feldspar), suggesting a granitic or feldspathic sedimentary source. Peak at 27.084° 2θ (d = 3.29 Å) shows highest intensity (1043 cps) with narrow FWHM (0.13°) suggesting a well-crystallized phase. Peak at 25.28° 2θ (d = 3.52 Å) indicates that the sample has moderate crystallinity while peak at 21.4° 2θ (d = 4.16 Å) implies broad peak (FWHM 2.9°) indicating poorer crystallinity or very fine particle size (29 Å crystallite size). The particle size distribution is equally observed in the diffraction pattern of CBNPs. The 29 Å crystallite size for the quartz/nacrite peak suggests nanocrystalline material or very fine clay particles. On the other hand, the 662 Å size for the 27° peak indicates larger crystalline domains (likely feldspars).

The high crystallinity and likely abundance of calcium-bearing minerals (e.g., $CaCO_3$) in CBNPs is expected to provide significant buffering capacity during anaerobic digestion. This is essential in maintaining optimal pH conditions (6.8 - 7.5) for methanogenic activity. Crystalline mineral phases contribute to neutralization of volatile fatty acids (VFAs), prevention of acidification and process inhibition and improved system resilience under high organic loading.

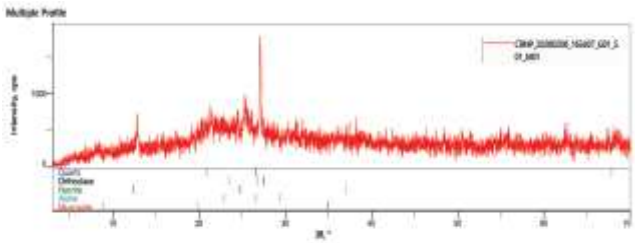

Figure 2: XRD analysis of CBNPs

3.1.4 Dynamic Light Scattering (DLS) of CBNPs

The DLS reports (Table 4) show that CBNPs weighted mean particle size of 87.16 nm. This shows that the sample is a nanoparticle since the particle size is less than 100 nm in agreement with the SEM results. Predominant particle size is 15.86 nm by intensity and 12.78 nm by volume distribution with minor aggregation. The PDI is 0.267 which lies in the range of 0.1 – 0.3, showing

that there is moderately narrow size distribution and the acceptable uniformity. This indicates that the sample prepared lies in the nano-scale and is suitable for the anaerobic digestion.

Table 4: Dynamic Light Scattering (DLS) results

Particle size distribution by intensity				Particle size distribution by volume		
Sample	Z-average Particle size (nm)	Dominat particle size (nm)	Polydisperity index (PDI)	Z-average Particle size (nm)	Dominat particle size (nm)	Polydisperity index (PDI)
CBNPs	87.16	15.86	0.267	87.16	12.78	0.267

3.1.5 XRF analysis of CBNPs

The XRF results shown in Table 5 confirms that CBNPs is more of aluminosilicate clay mineral. It is more abundant in SiO_2 and Al_2O_3 which are the components of nacrite. These two oxides form the structural backbone of clay. The stable Si-O-Si and Si-O-Al frameworks give the material its rigid, high surface area topography for microbial immobilization and anchor for slow-growing methanogens. Phosphorus in P_2O_5 is a macronutrient for microbial growth while iron in Fe_2O_3 is available as micronutrient and promotes DIET. In addition, Ca^{2+}, K^+ and Ti^{4+} ions drive cation exchange capacity. They can be exchanged to trap free ammonium ions ($NH_4^{+)}$ which can be harmful to the microbes and inhibitory to the process.

Table 5: XRF Analysis

Oxide	SiO_2	Al_2O_3	K_2O	CaO	TiO_2	P_2O_5	Fe_2O_3	MgO	**SO_3**	Cl	ZrO_2	PbO	Cr_2O_3
% comp	40.012	25.772	0.431	0.697	4.908	22.3499	3.317	0	0.618	0.898	0.206	0.03	0.058

3.2 Characterization results of the substrates

The result of the proximate analysis and the Physicochemical properties of the of the Substrates is shown in Table 6. The moisture content of the yam peels is in agreement with the result reported by Onu, Nweke and Nwabanne (2022). Yam peels has equally been consistently more acidic than the cow dung as reported in the literaure including Onu *et al.* (2022). In summary, the values in the Table are comparable and follow similar trends as the ones previously reported in the literature. For instance, yam peels have higher lignocellulosic fractions and ash content while cow dung has been reported to have higher nitrogen content. Cow dung supplies microbes and stabilizes pH. At 1:1 mixing ratio, the pH of the CD –YP mixture is obtained as the average (6.05). This pH is relatively favourable to the methanogens resulting to sustained methane yield. Also, high volatile solids (VS) content in yam peels increased the VS content of the cow dung to that of the mixture (25.84 %.) and hence, accelerates hydrolysis. Yam peels supply readily degradable carbohydrates; cow dung delivers diverse microbial consortia and buffering capacity. Together they balance C:N ratio and improve biodegradability compared to single substrates.

Table 6: Physicochemical properties of the substrates

Parameters	**Yam peel**	**Cow dung**
Moisture content (%)	56.217	66.154
Ash content (%)	3.869	1.113

pH	4.85	7.25
Total solids (%)	43.783	33.846
Hemicellulose (%)	20.765	11.855
Cellulose (%)	18.541	11.656
COD (mg/L)	480	320
Total Nitrogen (%)	1.232	3.192
Total organic carbon (%) blend	19.711	25.321
Total volatile solid (%)	36.399	15.278

3.3 Microbial Assay

Table 7 shows the bacteria present and those absent in a cow dung sample analyzed. According to DelaVega-Quintero *et al.* (2025). *Bacillus spp.* and *Pseudomonas aeruginosa* break complex organic polymers into simple soluble compounds. They secrete extracellular enzymes that break down cellulose, proteins, and fats into sugars, amino acids and fatty acids respectively. *Vibrio cholerae* and *E. coli* are the acidogenic bacteria identified in the sample; both convert the sugars (by fermentation) and amino acids to volatile fatty acids, hydrogen and carbon dioxide. *Pseudomonas aeruginosa* also plays a role in the acetogenesis step by converting organic monomers into fatty acids. Finally, methanogenic Archaea convert the acetic acid, hydrogen and carbon dioxide into methane.

Table 7: Microbial Assay results

Bacteria	**Status**	**Participatory stage**	**Min.Duration (days)**
Methanogenic Archaea	Present	Methanogenesis	5-10
Escherichia coli (E.coli)	Present	Acidogenesis/indicator of pathogen reduction	1-2
Salmonella enteric	Absent	-	-
Staphylococcus aureus	Absent	-	-
Bacillus spp	Present	Hydrolysis/acidogenesis	1-2
Mycobacterium tuberculosis	Absent	-	-
Pseudomonas aeruginosa	Present	Hydrolysis/ acidogenesis	1-2
Vibrio cholera	Present	Acidogenesis/indicator of pathogen reduction	1-2
Streptococcus pneumonia	Absent	-	-

3.4 GC analysis results of CBNPs

Table 8 shows that there were a lot of impurities in the biogas sample produced. This is not strange because the samples of biogas that was collected for the analyses was at the initial stage of the digestion. There were traces of acetate, acetic acid and others which are found in the acidogenesis, acetogenesis and methanogenesis stages of the anaerobic digestion process. They were possibly trapped in the produced biogas and can considerably reduce the flammability of the biogas. Hence, this necessitated the purification of the biogas samples to improve the flammability and calorific value. On the other hand, it was observed that the methane content from the CBNPs-enhanced process is higher than the one obtained in the blank. This is possibly due to the fact that the NPs adsorbed some of the inhibitors present in the system and consequently promoted the methane yield of the entire process in agreement with the report by Abdelsalam *et al.* (2016).

Table 8: Interpretation of the GC results

Sample	Methane (%)	CO_2 (%)	CO (%)	Acetic acid (%)	Hydrogen (%)	Ethyl acetate (%)	SO_2 (%)	Acetone (%)	O_2 (%)	Acetonitrile (%)	Methanol (%)
Blank	77.21	11.76	0.01	0.09	7.59	-	1.18	1.06	'-	1.10	0.09
CBNPs	80.26	11.68	0.31	0.30	3.57	1.18	0.41	0.05	2.25	-	-

3.5 ANOVA Study

In the ANOVA presented in Table 9, the model F-value is significant and shows that the whole model is valid and adequate to represent the data. This is validated by the fact that the p-value is significant ($p<0.05$), lack-of-fit p-value is insignificant, R^2 and predicted R^2 are close to 1. Also, the coefficient of variation is low showing that the data is accurate and can be reproduced.

The Table also revealed that all the p-values are less than the significance level (0.05). This implies that statistically, each factor has effect on the biogas yield independently as well as when combined with other factors. However, these effects could be synergistic or antagonistic.

Table 9: ANOVA Table

Source	Sum of Squares	df	Mean Square	F-value	p-value	
Model	9.885E+06	9	1.098E+06	199.83	< 0.0001	significant
A-Day	5.851E+05	1	5.851E+05	106.45	< 0.0001	
B-Nano. conc	1.554E+05	1	1.554E+05	28.27	0.0003	
C-Substr. ratio	6.934E+05	1	6.934E+05	126.15	< 0.0001	
AB	4.513E+05	1	4.513E+05	82.10	< 0.0001	
AC	1.051E+06	1	1.051E+06	191.26	< 0.0001	
BC	2.113E+05	1	2.113E+05	38.43	0.0001	
A^2	1.374E+06	1	1.374E+06	249.97	< 0.0001	
B^2	2.875E+06	1	2.875E+06	523.08	< 0.0001	
C^2	3.727E+06	1	3.727E+06	678.03	< 0.0001	
Residual	54963.68	10	5496.37			
Lack of Fit	54963.68	5	10992.74			
Pure Error	0.0000	5	0.0000			
Cor Total	9.940E+06	19				

3.6 Model Summary Statistics

The Predicted R^2 of 0.9531 is close to Adjusted R^2. This confirms the reliability and predictive capability of the model. Adequacy. The coefficient of variation indicates how the predicted values are scattered around the actual values. Its value is actually low indicating that there is minimal error in the prediction. The value of the standard deviation is equally good compared to the high value of the mean.

Table 10: Regression Statistics for RSM Model Performance

Std. Dev.	83.13	R^2	0.9955
Mean	1798.25	Adjusted R^2	0.9915
C.V. %	4.62	Predicted R^2	0.9634
		Adeq Precision	45.5292

3.7 RSM Model Equation and Interpretation of the Coefficients Involving CBNPs

A model equation was generated from the RSM. The model equation generated is quadratic showing the individual or interactive effects of the factors. It can be used to predict the biogas yields given the three factors considered. The model equation generated is given by:

$$Y = 2152.07 + 206.99A + 106.67B + 225.33C - 237.5AB + 362.5AC - 162.5BC + 308.77A^2 - 446.65B^2 - 508.52C^2 \quad (1)$$

The equation in terms of coded factors can be used to make predictions about the response for given levels of each factor. By default, the high levels of the factors are coded as +1 and the low levels are coded as -1. The coded equation is useful for identifying the relative impact of the factors by comparing the factor coefficients. The equation shows that all the factors have strong individual effects on biogas yield but substrates ratio has the strongest effect due to its largest positive coefficient. Also there is antagonistic or negative interaction between time and NPs concentration while there is moderate negative interaction between NPs concentration and substrates ratio. Negative quadratic terms for B and C indicate that the response Y will eventually decrease if any of the factors becomes too high. This means there is optimal value for each of them.

3.8 Cumulative Biogas Yields

Table 11 shows the cumulative biogas yield of 20 runs used in the experiment. Run 4, containing 150mg/L of CBNPs gave the highest yield, a cumulative biogas yield of 2150 ml in 9 days. The results show that CBNPs improved biogas production, This agrees with the findings by Hassanpourmoghadam *et al.* (2023). However, excessive NPs concentration led to reduced yield, consistent with the inhibitory effects reported by Kumar *et al.* (2021). In addition, from calculations, the RSM-prediction has a Mean Absolute Percentage Error (MAPE) of 4.35% and a Root-Mean-Square Error of 58.78. The low values of MAPE and RSME indicates that the RSM model can predict the process with high accuracy.

Table 11: Comparison of the Experimental and RSM predicted Biogas Yields with the

Run	A:Time (Days)	B:Nano. Conc. (mg/L)	C: Substr. Ratio (%)	Exptal Biogas yield (ml)	RSM-Predicted yield
1	12	200	75	1300	1390
2	12	100	75	2050	1976
3	6	200	75	750	726
4	9	150	50	2150	2152
5	6	200	25	1200	1325
6	12	100	25	400	476
7	6	100	75	300	362
8	9	150	50	2150	2152
9	9	150	8	400	335
10	9	150	50	2150	2152

11	6	100	25	350	312
12	4	150	50	980	931
13	9	66	50	700	709
14	12	200	25	550	539
15	9	150	50	2150	2152
16	9	150	50	2150	2152
17	9	150	92	1100	1093
18	14	150	50	1650	1627
19	9	234	50	1150	1068
20	9	150	50	2150	2152

3.9 3D Plots

Figure 3(a) represents the interaction between digestion time and nanoparticle concentrations. The convex shape with a peak region shows that the model is quadratic and confirms the presence of an optimum operating condition. It equally shows that both linear and quadratic effects are significant. The biogas yield increases with both digestion time and nanoparticle concentration initially at constant substrate ratio of 1:1. The biogas yield increased with digestion time up to approximately 10 – 11 days, after which there was a decline, possibly due to substrate depletion and reduced microbial activity. Similarly, NPs concentration showed a positive effect up to approximately 100 – 150 mg/L. Beyond this range, further increases led to a decrease in biogas yield which is in accordance with the result obtained by Abdelsalam *et al.* (2016). These led to increase in biogas yield up to a maximum yield of about 2238.28 ml. afterwards, there was decrease in yield. The NPs concentration that gave this yield is 151 mg/L substrates in about 11 days.

On the other hand, Figure 3(b) shows the combined effect of both time and substrates ratio at constant NPs concentration of 151 mg/L. Initially, there was increase in biogas yield up to a maximum yield of about 2238.28 ml, afterwards, there was decrease in the yield, possibly due to increased inhibition and formation of scum by cow dung. The substrate ratio that gave this yield is 56% (1:1) in 11 days.

Figure 3(c) shows that there is a strong interaction between the NPs concentration and substrates ratio. Both must be maintained at a particular range for optimal yield at constant time.

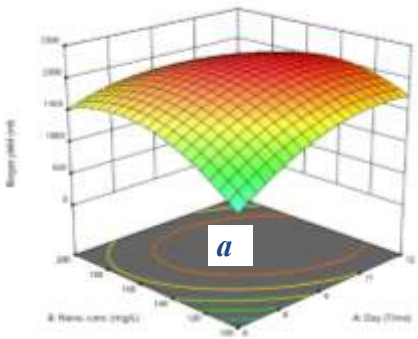

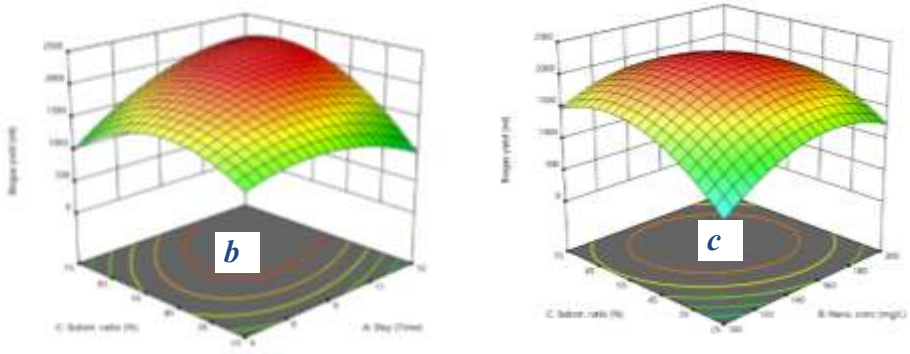

Figure 3(a-c): 3D interaction of the various factors that affect the biogas yield

4.0 Conclusions

This study investigated the impact of clay-based nanoparticles on biogas yield from anaerobic co-digestion of cow dung and yam peels.

The research employed experimental anaerobic digestion and RSM. The results demonstrated that the addition of nanoparticles significantly improved biogas and methane yields compared to the control (without nanoparticles). This improvement is attributed to enhanced microbial activity, improved electron transfer, and accelerated degradation of complex organic substrates. Among the tested conditions, an optimum range of substrate composition, retention time, and nanoparticle dosage was identified through RSM optimization, leading to maximum methane production efficiency. The optimum value of the biogas yield was 2265 ml, while the optimal factors were Time (11 days), Substrates mixing ratio (64% or CD: YP ratio of 16:25) and NPs concentration (144 mg/L). In addition, experimental results revealed that there was 24.5 % increase in biogas yield and 4.0% increase in the methane content when CBNPs was employed in the co-digestion of CD and YP compared to when there was no addition of NPs

Funding

This research received no external funding

Acknowledgments

My gratitude goes to Dr. C.C. Okoye, the head of the department and Dr. M.N. Abonyi for their immense contribution to the success of this publication

Conflicts of Interest

The Authors declare no conflict of interest.

References

Abdelsalam, E. and Samer, M. (2019). Biostimulation of anaerobic digestion using nanomaterials for increasing biogas production. *Reviews in Environmental Science and Bio/Technology, 18*, 525-541.

Abdelsalam, E., Samer, M., Attia, Y., Abdel-Hadi, M., Hassan, H. and Badr, Y. (2016). Comparison of nanoparticles effects on biogas and methane production from anaerobic digestion of cattle dung slurry. *Renewable energy, 87*, 592-598.

Abdelsalam, E., Samer, M., Attia, Y., Abdel-Hadi, M., Hassan, H. and Badr, Y. (2019). Effects of laser irradiation and Ni nanoparticles on biogas production from anaerobic digestion of slurry. *Waste and Biomass Valorization, 10*, 3251-3262.

Abdelwahab, T. A. M., Mohanty, M. K., Sahoo, P. K., Behera, D. and Fodah, A. E. M. (2021). Cobalt nanoparticles to enhance anaerobic digestion of cow dung: focusing on kinetic models for biogas yield and effluent utilization. *Biomass Conversion and Biorefinery, 13*(13), 11657-11669.

Ajayi-Banji, A., Pourhashem, G., Rahman, S. and Feng, X. (2024). Evaluating the environmental impacts of pretreatment and nanoparticles in solid-state anaerobic digestion using life cycle assessment. *Energy Research, 17*(3), 1971-1984.

Castro, J. C. d., Resende, E., Taveira, I., Enrich-Prast, A. and Abreu, F. (2024). Nanotechnology boosts the production of clean energy via nanoparticle addition in anaerobic digestion. *Frontiers in Nanotechnology, 6*, 1406344.

DelaVega-Quintero, J. C., Nuñez-Pérez, J., Lara-Fiallos, M., Barba, P., Burbano-García, J. L. and Espín-Valladares, R. (2025). Advances and Challenges in Anaerobic Digestion for Biogas Production: Policy, Technological, and Microbial Perspectives. *Processes, 13*(11), 3648.

Farghali, M., Andriamanohiarisoamanana, F. J., Ahmed, M. M., Kotb, S., Yamamoto, Y., Iwasaki, M., Yamashiro, T. and Umetsu, K. (2020). Prospects for biogas production and H2S control from the anaerobic digestion of cattle manure: The influence of microscale waste iron powder and iron oxide nanoparticles. *Waste Management, 101*, 141-149.

François, M., Lin, K.-S., Rachmadona, N. and Khoo, K. S. (2023). Advancement of nanotechnologies in biogas production and contaminant removal: A review. *Fuel, 340*, 127470.

Hassanpourmoghadam, L., Goharrizi, B. A., Torabian, A., Bouteh, E., Rittmann, B. E. and Bioenergy. (2023). Effect of Fe3O4 nanoparticles on anaerobic digestion of municipal wastewater sludge. *Biomass, 169*, 106692.

Jozanikohan, G. and Abarghooei, M. N. J. J. o. P. E. (2022). The Fourier transform infrared spectroscopy (FTIR) analysis for the clay mineralogy studies in a clastic reservoir. *Journal of Petroleum Exploration and Production Technology, 12*(8), 2093-2106.

Khan, S. and Hossain, M. K. (2022). Classification and properties of nanoparticles. In *Nanoparticle-based polymer composites* (pp. 15-54): Elsevier.

Kumar, M., Dutta, S., You, S., Luo, G., Zhang, S., Show, P. L., Sawarkar, A. D., Singh, L. and Tsang, D. C. (2021). A critical review on biochar for enhancing biogas production from anaerobic digestion of food waste and sludge. *Journal of Cleaner Production, 305*, 127143.

Lohani, S. P. and Havukainen, J. (2018). Anaerobic digestion: factors affecting anaerobic digestion process. *Waste bioremediation*, 343-359.

Obaideen, K., Abdelkareem, M. A., Wilberforce, T., Elsaid, K., Sayed, E. T., Maghrabie, H. M. and Olabi. (2022). Biogas role in achievement of the sustainable development goals: Evaluation, Challenges, and Guidelines. *Journal of the Taiwan Institute of Chemical Engineers, 131*, 104207.

Onu, C. E., Nweke, C. N. and Nwabanne, J. T. (2022). Modeling of thermo-chemical pretreatment of yam peel substrate for biogas energy production: RSM, ANN, and ANFIS comparative approach. *pplied Surface Science Advances, 11*, 100299.

Park, J.-H., Kang, H.-J., Park, K.-H. and Park, H.-D. (2018). Direct interspecies electron transfer via conductive materials: A perspective for anaerobic digestion applications. *Bioresource Technology, 254*, 300-311.

Passalacqua, E., Collina, E., Fullana, A. and Mezzanotte, V. (2024). Mini-review: Nanoparticles for enhanced biogas upgrading. *Waste Management Research*, 0734242X241231397.

Teğin, İ. and Saka, C. (2023). Chemical and thermal activation of clay sample for improvement adsorption capacity of methylene blue. *International Journal of Environmental Analytical Chemistry, 103*(16), 4503-4514.

Tzenos, C. A., Kalamaras, S. D., Economou, E.-A., Romanos, G. E., Veziri, C. M., Mitsopoulos, A., Menexes, G. C., Sfetsas, T. and Kotsopoulos, T. A. (2023). The Multifunctional Effect of Porous Additives on the Alleviation of Ammonia and Sulfate Co-Inhibition in Anaerobic Digestion. *Sustainability, 15*(13), 9994.

Umeghalu, C., Chukwuma, E., Okonkwo, I. and Umeh, S. (2012). Potentials for biogas production in Anambra State of Nigeria using cow dung and poultry droppings. *International Journal of Veterinary Science, 1*(1), 25-29.

Vannarath, A., Ahmad, Y. H., Farhat, T. M., Chae, K.-J., Aljaber, A. S. and Al-Qaradawi, S. Y. (2025). Insights into the addition of exogenous materials to enhance anaerobic digestion. *Energy Conversion and Management, 27*, 101078.

Zhang, C., Xiao, G., Peng, L., Su, H. and Tan, T. (2013). The anaerobic co-digestion of food waste and cattle manure. *Bioresource Technology, 129*, 170-176.